Intrinsic Charge Transport on the Surface of Organic Semiconductors

V. Podzorov,[1,*] E. Menard,[2] A. Borissov,[1] V. Kiryukhin,[1] J. A. Rogers,[2] and M. E. Gershenson[1]
[1]*Department of Physics and Astronomy, Rutgers University, Piscataway, New Jersey, USA*
[2]*Department of Materials Science and Engineering, University of Illinois, Urbana-Champaign, Illinois, USA*
(Received 23 March 2004; published 20 August 2004)

The air-gap field-effect technique enabled realization of the intrinsic (not limited by static disorder) polaronic transport on the surface of rubrene ($C_{42}H_{28}$) crystals over a wide temperature range. The signatures of this intrinsic transport are the anisotropy of the carrier mobility, μ, and the growth of μ with cooling. Anisotropy of μ vanishes in the activation regime at low temperatures, where the transport is dominated by shallow traps. The deep traps, introduced by x-ray radiation, increase the field-effect threshold without affecting μ, an indication that the filled traps do not scatter polarons.

DOI: 10.1103/PhysRevLett.93.086602 PACS numbers: 72.80.Le, 71.38.Ht

One of the problems of experiments with organic semiconductors is realization of the *intrinsic, not limited by static disorder* charge transport. The difficulty of its demonstration is related to the polaronic nature of the charge carriers in organic molecular crystals (see, e.g., [1]): small polarons can be trapped by numerous types of crystal defects. The benchmark in the study of the intrinsic transport has been established in time-of-flight (TOF) experiments [2], which probe the charge transport in the bulk ultrapure organic crystals at small carrier densities. The intrinsic transport in TOF experiments is characterized by an increase of the carrier mobility, μ, with cooling and a pronounced anisotropy of μ. Theoretical treatment of these results was based on the Holstein concept of small polarons (see, e.g., [1,3]).

Until recently, the experimental tool used to probe the intrinsic charge transport on the *surface* of organic semiconductors was unavailable: the current flow in the organic thin-film transistors (TFTs) is typically dominated by disorder [4]. Fabrication of the single-crystal organic field-effect transistors (OFETs) (see, e.g., [5,6]) provides an opportunity to study the charge transport on the organic surface with significantly reduced disorder. It also offers a possibility to explore the regime of high charge densities, many orders of magnitude greater than in the TOF experiments, which may lead to observation of new electronic phases. However, despite recent technological advances, realization of the intrinsic transport on the organic surface remains a challenge because the concentration of defects at the surface is typically higher than in the bulk.

In this Letter, we report on the observation of the intrinsic transport of field-induced charges on the surface of single crystals of rubrene ($C_{42}H_{28}$). Application of a novel experimental technique based on the "air-gap" transistor stamps [7] allowed realization of a high mobility of *p*-type carriers, $\mu(300\ \mathrm{K}) \sim 20\ \mathrm{cm}^2/\mathrm{V\,s}$. Two signatures of the intrinsic transport—the mobility increase with decreasing temperature and the mobility anisotropy—have been observed in the temperature range ~150–300 K. At lower temperatures, where the charge transport is dominated by shallow traps, μ decreases exponentially with cooling and its anisotropy vanishes.

The single crystals of rubrene have been grown from the vapor phase [5]. We have used the transistor stamps based on elastomeric polydimethylsiloxane (PDMS) substrates with a surface relief pattern (see the inset of Fig. 1) [7]. The continuous metal film, deposited on the stamp by thermal evaporation of gold, breaks at the vertical walls of the pattern imprinted on the PDMS surface: this produces the electrically isolated source, drain, and gate electrodes. The gate is recessed from the level of the source and drain pads by 3 to 5 μm. Fabrication of the field-effect structures is completed after the organic crystal is laminated against the surface of the stamp [8]. The

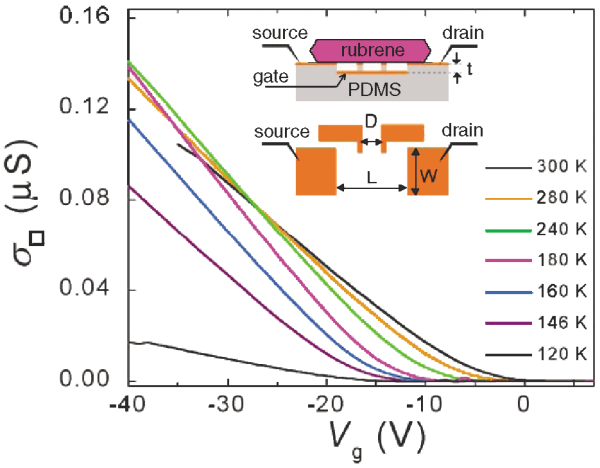

FIG. 1 (color online). The surface conductivity, $\sigma_\square$, as a function of the gate voltage, V_g, measured with the 4-probe air-gap transistor stamp along the *b* axis of rubrene (the source-drain voltage $V_{SD} = 5$ V, the drain is grounded). The inset schematically shows the transistor stamp: $L = 0.75$ mm, $D = 0.25$ mm, $W = 1.25$ mm, $t = 5$ μm; $C_i = 0.2\ \mathrm{nF/cm}^2$.

stamp does not touch the crystal surface within the area of the conduction channel; this allows minimization of the density of surface defects introduced in the process of FET fabrication. The electrical breakdown strength of these structures in air is very high ($\geq 1.5 \times 10^5$ V/cm), which is consistent with Paschen's law for a micron-size separation between the gate and the channel (see, e.g., [9]).

The charge carriers are injected in OFETs through the Schottky barriers at the metal/organic interface [10]. In order to exclude the contact effects, we have used the 4-probe configuration [5]. Figure 1 shows the dependence of the sheet conductance $\sigma_\square = (D/W)(I_{SD}/V)$ on the gate voltage V_g measured at a constant source-drain voltage V_{SD} (I_{SD} is the source-drain current, V is the voltage difference between the voltage probes separated by a distance D, and W is the channel width). At large V_g, the dependences $\sigma_\square(V_g)$ are linear: this regime corresponds to the V_g-independent mobility of carriers $\mu = \sigma_\square/en$ (n is the two-dimensional density of mobile field-induced carriers). The carrier mobility in the linear regime is proportional to the slope of $\sigma_\square(V_g)$ dependences, $\mu = (1/C_i)(d\sigma/dV_g)$ [11], where C_i is the specific capacitance between the gate and the channel (the gate dielectric is air or vacuum, depending on the experimental conditions). For the estimate of μ, we have used the capacitance 0.2 nF/cm^2 calculated from the device geometry; this value is consistent with the direct measurements of C_i in the test structures formed by lamination of the stamp against a metallic surface [7]. This definition of μ assumes that all carriers with the density $n = [C_i(V_g - V_g^{th})]/e$, induced by the transverse electric field above the threshold, are mobile and their energies are within the highest occupied molecular orbital (HOMO) band. A weak dependence $\mu(V_g)$ observed for our field-effect structures justifies this assumption. For comparison, the mobility in organic TFTs [12] and amorphous silicon (α-Si:H) FETs [13] are strongly V_g dependent; in the latter case, the density of localized states is so high that the Fermi level at the surface remains below the bottom of the conduction band even at largest V_g, and the conduction is governed by the multiple trap and release (MTR) mechanism.

Figure 1 shows the evolution of the $\sigma_\square(V_g)$ dependences measured along the b axis of rubrene with decreasing temperature. The mobility, proportional to the slope $d\sigma_\square/dV_g$, initially increases, reaches a maximum at $T \sim 150$ K, and decreases rapidly with further cooling (see also Fig. 2). The mobility measured along the a axis is found to be systematically lower by a factor of 2.5–3 at 300 K, in line with our recent study [14]; this anisotropy is due to a stronger π-π overlap in the b direction in rubrene crystals (the molecular packing is shown in the inset of Fig. 3). The mobility anisotropy persists with cooling down to $T \sim 150$ K. The increase of the field-effect threshold with decreasing temperature

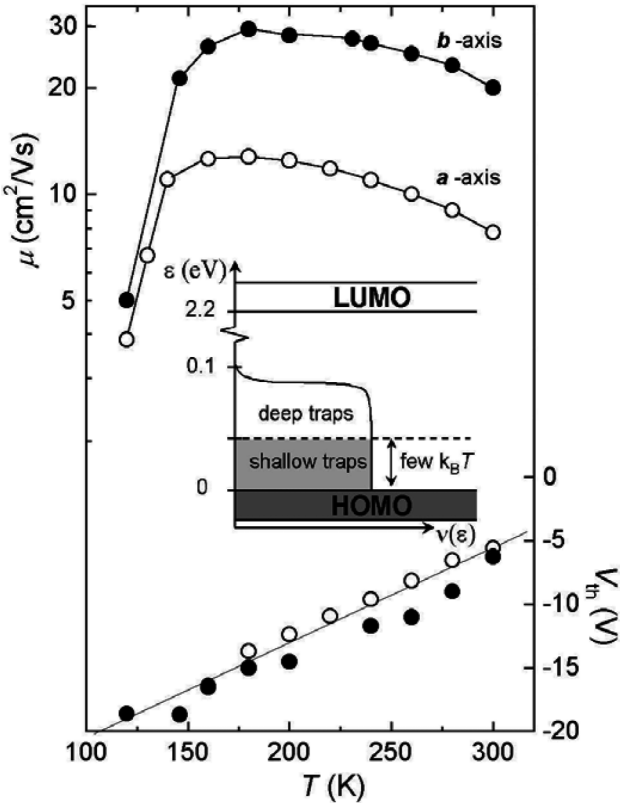

FIG. 2. The temperature dependence of the field-effect mobility and the threshold voltage measured along the a and b axes of rubrene crystals. The inset schematically shows the electronic states near the HOMO energy.

(Figs. 1 and 2) precludes measurements of μ below 100 K [15].

On the basis of our results, we can qualitatively reconstruct the energy diagram of the electronic states near the HOMO level in the studied rubrene crystals (see the inset of Fig. 2). Within the HOMO-LUMO (lowest unoccupied molecular orbital) gap, there are localized electronic states (traps) associated with the crystal defects, such as chemical impurities, structural disorder, and surface states. Injection of p-type carriers results in filling the traps and shifting the Fermi energy at the organic surface, E_F, towards the HOMO level. Below the field-effect threshold ($|V_g| < |V_{th}|$), the injected charge is trapped in the localized states with energies separated by more than a few k_BT from the HOMO level (the *deep* traps). When the Fermi level reaches the traps with energies within a few k_BT from the HOMO level (the *shallow* traps), the surface conductivity increases dramatically by many orders of magnitude, owing to the thermal excitation of the carriers from the shallow traps to the HOMO level.

With cooling, the borderline between deep and shallow traps shifts towards HOMO. The concentration of deep traps with energies $\geq$ few k_BT above the HOMO level, $N_{tr} = (C_i V_{th})/e$, increases from 0.7×10^{10} cm^{-2} at 300 K to 2×10^{10} cm^{-2} at 150 K. Interestingly, the quasilinear

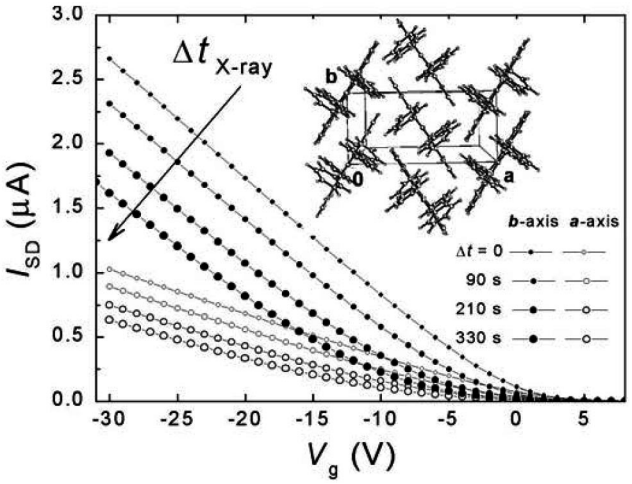

FIG. 3. The effect of the x-ray radiation on OFET characteristics. $I_{SD}(V_g)$ have been measured simultaneously along the a and b axes using a 2-probe transistor stamp with two perpendicular channels. After each x-ray exposure, the crystal was measured at 300 K in air and in the dark; Δt indicates the cumulative exposure time. The mobility proportional to the slope of $I_{SD}(V_g)$ is not affected by x-ray irradiation, whereas V_{th} is noticeably increased.

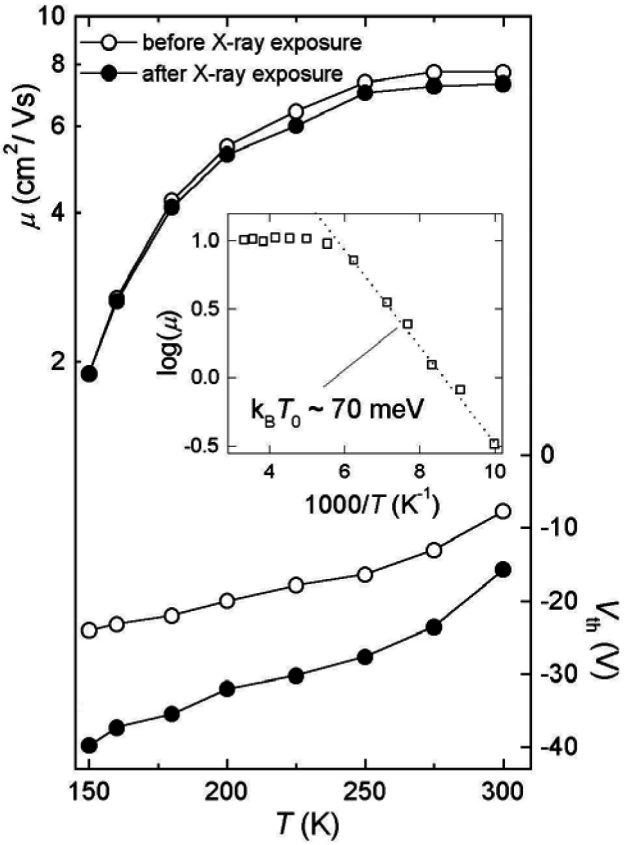

FIG. 4. The temperature dependence of the field-effect mobility $\mu(T)$ and the threshold voltage $V_{th}(T)$ of the rubrene OFET measured by the 4-probe transistor stamp along the b axis before (open circles) and after (solid circles) the x-ray exposure for $\Delta t = 4$ min. The inset is the dependence $\mu(T)$ along the b axis for another device (not exposed to x rays): the low-T fit is the Arrhenius dependence with the activation energy ~70 meV.

increase of V_{th} with cooling (see Fig. 2) indicates that the energy distribution of trap states, $\partial N_{tr}/\partial E = (C_i/k_B e) \times (\partial V_{th}/\partial T) \approx 10^{12}$ cm^{-2} eV^{-1}, is almost energy independent within ~0.1 eV near the HOMO band.

The $\mu(T)$ dependences measured along the a and b axes are shown in Fig. 2. The value of $\mu^{\mathbf{b}}(300\text{ K}) \sim 20$ cm^2/V s in rubrene exceeds by a factor of 10 $\mu(300\text{ K})$ observed in the TOF experiments with naphthalene and anthracene [2]. This high mobility is not unique: the values of μ for most of the studied crystals were within the interval 15–20 cm^2/V s. Note that the electric field along the conduction channel in our experiment (~50 V/cm) is by several orders of magnitude smaller than that in the TOF measurements. Therefore, detrapping due to the large drag fields can be neglected.

Two transport regimes are clearly seen in Fig. 2: (i) at high temperatures (150–300 K), the mobility is strongly anisotropic and increases with cooling; (ii) at $T < 150$ K, the mobility rapidly decreases with cooling, and the anisotropy of μ vanishes. The low-temperature drop of the mobility can be fitted by an Arrhenius dependence $\mu(T) = \mu_0 \exp(-T_0/T)$ with the activation energy $k_B T_0 \sim 70$ meV, which is the same for both crystallographic directions (see also the inset of Fig. 4). We argue that the former regime corresponds to the intrinsic polaronic transport, whereas at low temperatures the transport is dominated by the multiple trapping and releasing of carriers by shallow traps [12]. Typically, the increase of μ with cooling is observed for the devices with $\mu^{\mathbf{b}}(300\text{ K}) \geq 10$ cm^2/V s. For the devices with $\mu^{\mathbf{b}}(300\text{ K}) < 10$ cm^2/V s (which constitute a small fraction of all studied devices), μ is almost T independent at high T, and exponentially decreases at lower T with T_0 similar to that for the higher-μ devices (Fig. 4).

Observation of the intrinsic transport at high T does not imply that the trapping is completely eliminated. On the contrary, the higher the temperature, the higher the total number of shallow traps involved in the trap-and-release processes. However, at high enough T, the time that a polaron spends within a shallow trap with energy E_{tr}, $\tau_{tr} \propto \exp(E_{tr}/k_B T)$, can be much smaller than the time it propagates between the traps, τ. In this case ($\tau_{tr} \ll \tau$), the effective drift mobility in the MTR model [16], $\mu_{eff} = \mu_0(\tau/\tau + \tau_{tr})$, is reduced to the intrinsic (trap-free) mobility μ_0. In the opposite limit ($\tau_{tr} \gg \tau$), the charge transport is dominated by trapping and $\mu_{eff} = \mu_0(\tau/\tau_{tr}) \propto \exp(-E_{tr}/k_B T)$. This regime is observed for the studied OFETs at $T < 150$ K. Note that the crossover from the intrinsic to the thermally activated transport in the bulk has been observed in the TOF measurements of organic crystals [17] with *ppm* impurity concentrations

that are close to the trap density in the studied rubrene crystals.

Our experiments show that the mobility anisotropy vanishes in the trap-dominated regime (Fig. 2). This observation is consistent with the MTR model. Indeed, the time of propagation of the carrier between the traps, τ, is inversely proportional to the intrinsic mobility in the direction of propagation (e.g., $\tau^{\mathbf{b}} \propto 1/\mu_{\mathbf{0}}{}^{\mathbf{b}}$). Thus, for an isotropic distribution of traps in the crystal, one might expect vanishing of the anisotropy of μ_{eff} in the regime $\tau_{\text{tr}} \gg \tau$.

In order to better understand charge trapping, we deliberately introduced defects in the rubrene crystals by exposing them to the x-ray radiation [18]. The ionizing radiation breaks the molecules and produces new chemical species that act as local defects in the crystal structure [19]. The trans-conductance characteristics of the rubrene OFET measured along the *a* and *b* axes before and after the x-ray exposure are shown in Fig. 3; the corresponding $\mu(T)$ and $V_{\text{th}}(T)$, measured by the 4-probe technique, are shown in Fig. 4. The x-ray treatment significantly increases V_{th} and thus the density of deep traps, without affecting $\mu(T)$. This indicates that (i) the x ray does not create traps within $\sim$0.1 eV from the HOMO level (shallow traps) and (ii) the deep traps, being filled above the threshold, do not affect the motion of mobile polaronic carriers.

To summarize, we have studied the transport of *p*-type polaronic carriers on the surface of single crystals of rubrene by the air-gap field-effect transistor stamps. This technique allowed us to minimize the density of surface defects/traps and to realize the intrinsic polaronic transport on the surface of organic semiconductors. Two transport regimes have been identified: (i) the intrinsic regime observed at high temperatures, where the mobility is anisotropic and increases with decreasing temperature, and (ii) the shallow-trap-dominated regime, where the mobility decreases rapidly with cooling and the anisotropy of mobility vanishes. Our experiments with x-ray irradiation of organic crystals show that the filled deep traps do not contribute to the scattering of polarons.

This work at Rutgers was supported by the NSF Grants No. DMR-0405208 and No. ECS-0437932.

*Electronic address: podzorov@physics.rutgers.edu

[1] E. A. Silinsh and V. Čapek, *Organic Molecular Crystals: Interaction, Localization, and Transport Phenomena* (AIP Press, New York, 1994).
[2] N. Karl *et al.*, J. Vac. Sci. Technol. A **17**, 2318 (1999); N. Karl, in *Organic Electronic Materials*, edited by R. Farchioni and G. Grosso (Springer, Berlin, 2001), pp. 215–239, 284–326.
[3] K. Hannewald and P. A. Bobbert, Phys. Rev. B **69**, 075212 (2004).
[4] S. F. Nelson *et al.*, Appl. Phys. Lett. **72**, 1854 (1998); G. Horowitz, Adv. Mater. **10**, 365 (1998).
[5] V. Podzorov, V. M. Pudalov, and M. E. Gershenson, Appl. Phys. Lett. **82**, 1739 (2003); V. Podzorov *et al.*, Appl. Phys. Lett. **83**, 3504 (2003).
[6] R. W. I. de Boer *et al.*, Phys. Status Solidi (a) **201**, 1302 (2004).
[7] E. Menard *et al.* (to be published).
[8] Assembling of the rubrene FETs was performed in air; no degradation of the device performance was noticed after prolonged storage of the crystals in air and in the dark.
[9] T. Ono, D. Y. Sim, and M. Esashi, J. Micromech. Microeng. **10**, 445 (2000).
[10] A. B. Chwang and C. D. Frisbie, J. Phys. Chem. B **104**, 12 202 (2000); R. A. Street and A. Salleo, Appl. Phys. Lett. **81**, 2887 (2002); G. B. Blanchet *et al.*, Appl. Phys. Lett. **84**, 296 (2003).
[11] S. M. Sze, *Physics of Semiconductor Devices* (Wiley, New York, 1981).
[12] G. Horowitz *et al.*, J. Appl. Phys. **87**, 4456 (2000).
[13] M. Shur, M. Hack, and J. G. Shaw, J. Appl. Phys. **66**, 3371 (1989).
[14] V. C. Sundar *et al.*, Science **303**, 1644 (2004).
[15] The field-effect threshold V_{th} is determined as the voltage of the interception of linear interpolation of $\sigma(V_g)$ curve and V_g axis.
[16] R. H. Bube, *Photoconductivity in Solids* (Wiley, New York, 1960).
[17] D. C. Hoesterey and G. M. Letson, J. Phys. Chem. Solids **24**, 1609 (1963); K. H. Probst and N. Karl, Phys. Status Solidi (a) **27**, 499 (1975).
[18] Radiation source: Cr x-ray tube, $V = 20$ kV, $I = 10$ mA, source-sample distance 15 cm.
[19] *Radiation Chemistry*, edited by Farhataziz and M. A. J. Rodgers (VCH Publishers, New York, 1987).